Physica E: Low-dimensional Systems and Nanostructures 114 (2019) 113629

Contents lists available at ScienceDirect

Physica E: Low-dimensional Systems and Nanostructures

journal homepage: www.elsevier.com/locate/physe

Electron transfer from the barrier in InAs/GaAs quantum dot-well structure

I. Filikhin[a,*], Th. Peterson[a], B. Vlahovic[a], S.P. Kruchinin[b], Yu.B. Kuzmichev[c], V. Mitic[d]

[a] North Carolina Central University, CREST Center, 1801 Fayetteville St., 27707 Durham, USA
[b] Bogolyubov Institute for Theoretical Physics, NASU 14-b, Metrolohichna Str., Kiev 03143, Ukraine
[c] Yaroslavl State Pedagogical University, 108 Respublikanskaya St., 150000 Yaroslavl, Russia
[d] University of Niš, Faculty of Electronic Engineering, Aleksandra Medvedeva 14, Niš, Serbia

ARTICLE INFO

Keywords:
Quantum wells
Quantum dots
Single electron levels
Tunneling localization

ABSTRACT

We study single electron tunneling from the barrier in the binary InAs/GaAs quantum structure, including quantum well (QW) and quantum dot (QD). Tunneling is described in the terms of localized/delocalized states and their spectral distributions. Modeling is performed using the phenomenological effective potential approach for InAs/GaAs heterostructures. The results for the two and three-dimensional models are presented, focused on the effect of QD-QW geometry variations. The relation to the PL experiments is shown.

1. Introduction

Weakly coupled binary semiconductor nanoscale systems demonstrate perspectives for nano-sensor applications, due to high sensitivity of electron localization and resonance tunneling, between the objects of the system, on symmetry violation [1,2]. The single electron tunneling properties of one dimensional (1D), 2D, and 3D structures as well as double quantum wells (DQWs), double quantum dots (DQDs), and double quantum rings (DQRs) are well known. The electron spectra of such quantum objects, two- and three dimensional (2D and 3D) were studied previously [3] in relation to the electron localizations and tunneling between the objects. The wave function of electron may be localized in one of the nanostructures or be delocalized when it is spread over the whole system. Tunneling occurs in the last case. Under condition of weak coupling objects, electron wave function can be localized in both objects but with different probability. We explore experimental possibility for optical registration of electron localizations in binary quantum systems. In this work we are focused on the resonance tunneling in 3D/1D and 2D/1D nanoscale InAs/GaAs dot-well complex. This complex has a mixed spectral structure: discrete spectrum for QD (in 3D and 2D) and continuous spectrum for QW when QW is considered in three- or two-dimensional space [4–6]. Our modeling of carrier transfer from the barrier in InAs/GaAs dot-well tunnel-injection structure is performed using a band gap model based on the effective potential [7–9]. It has to be stressed that the tunneling is described in the terms of localized/delocalized states and their spectral distribution [3]. Results are compared with the main effect of the optical PL experiments given by Yu. I. Mazur et al. [10].

2. Model

Presented work was motivated by the experimental results of coherent coupling between photo-excited quantum-dots and a quantum well reported in Refs. [10–14]. The schematic explanation of the PL experiments [10] is given in Figs. 1 and 2. The coupling in the QD-QW complex was investigated in work [10], studying the dependence of quantum-dot photoluminescence as a function of quantum dot-well barrier thickness. It was shown that the resonant tunneling rate depends on the effective barrier thickness. This strongly affects the exciton dynamics in these hybrid structures as compared to isolated QW and QD. A specific behavior of the communication between a quantum-dot and quantum well was discussed in Refs. [13,14]. The InAs/GaAs quantum heterostructure is modeled using an effective potential model. The effective potential simulates the strain effect in the InAs/GaAs heterostructures [7–9]. The band gap model for description of the QDs (and QWs) is presented in Fig. 3. Here, the effective potential is given by V_s and the band gap potential is V_c. The InAs/GaAs heterostructure is modeled [7] utilizing a ***kp***-perturbation single sub-band approach. The problem is mathematically formulated by the Schrödinger equation in two (three) dimensions:

$$(\hat{H}_{kp} + V_c(r) + V_s(r))\Psi(r) = E\Psi(r).$$

Here $\hat{H}_{kp}$ is the single band ***kp***-Hamiltonian operator $\hat{H}_{kp} = -\nabla\frac{\hbar^2}{2\,m^*}\nabla$, $m^* = m^*(r)$ is the electron effective mass which depends on the position of the electron, and $V_c(r)$ is the band gap potential. $V_c(r) = 0$ inside the QD (QR), and is equal to V_c outside the QD (QR), where V_c is defined by the conduction band offset for the bulk. The band gap potential for the

* Corresponding author.
E-mail address: ifilikhin@nccu.edu (I. Filikhin).

https://doi.org/10.1016/j.physe.2019.113629
Received 19 April 2019; Received in revised form 11 June 2019; Accepted 9 July 2019
Available online 18 July 2019
1386-9477/

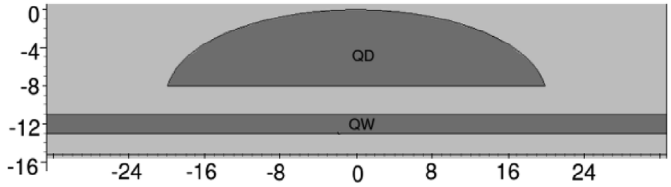

Fig. 1. Geometry of the QD-QW complex (cross section). The sizes are given in nm. The profile of the fabricated QD is presented in Ref. [12].

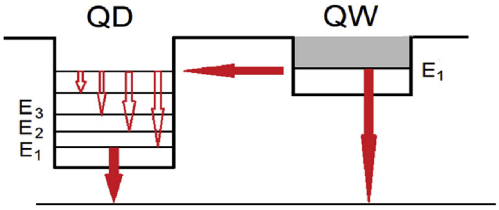

Fig. 2. Schematic description of the electron confinement structure and energy levels for the PL experiments presented in Ref. [10]. The tunneling between QD and QW is shown by a horizontal arrow. The vertical arrows correspond to excitons. Open arrows show the transitions between levels.

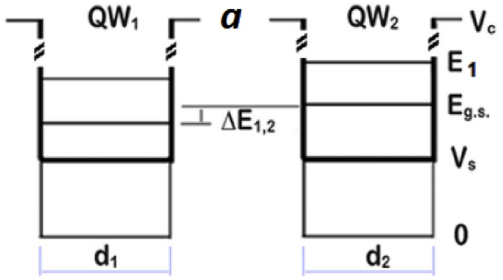

Fig. 3. Band gap model for InAs/GaAs double quantum well (in 1D). The system includes two quantum wells, QW_1 and QW_2, which differ by sizes d_1 and d_2. The barrier thicknesses is a.

conduction band is chosen as $V_c = 0.594$ eV. Bulk effective masses of InAs and GaAs are $m_1^* = 0.024m_0$ and $m_2^* = 0.067m_0$, respectively, where m_0 is the free electron mass. $V_s(r)$ is the effective potential simulating the strain effect, it has an attractive character and acts inside the volume of the QD [7,8]. The magnitude of the potential can be chosen to reproduce experimental data. For example, the magnitude of V_s for the conduction band chosen in Ref. [8] is 0.31 eV.

We consider a QD-QW complex as two-level quantum system [15] and describe the electron tunneling in the system within terminology of spectral distributions of the localized/delocalized states [1].

Double quantum dot is an example of the two-level quantum systems. The spectrum of single electron confinement states in DQDs is a set of quasi-doublet levels. The electron can be localized in one of the quantum dots or be delocalized over both QDs. The electron tunneling between QDs in DQD is reflected in the electron localization. The tunneling occurs through the anti-crossing of levels and, in case of identical QDs, is extremely sensitive on the shape symmetry violation of the systems [1,3]. To evaluate the electron localization one can use the electron average coordinate $\langle x\rangle$, which is calculated as: $\langle x\rangle = \langle\Psi|x|\Psi\rangle$, where Ψ is wave function of the system. In approach of the two-level system, Ψ is represented by superposition of the wave functions ψ_1 and ψ_2 of separated left (1) and right (2) quantum dots. The x-coordinate origin is the mid-point of the two QWs. The average coordinates $\langle x\rangle_+$ and $\langle x\rangle_-$, for the electron wave functions of the quasi-doublet, Ψ_+ and Ψ_-, can be written as:

$$\langle x\rangle_+ = -\cos^2(\Theta/2)|\langle x\rangle_1| + \sin^2(\Theta/2)|\langle x\rangle_2| + 2\sin(\Theta/2)\cos(\Theta/2)|\langle x\rangle_{12}|,$$

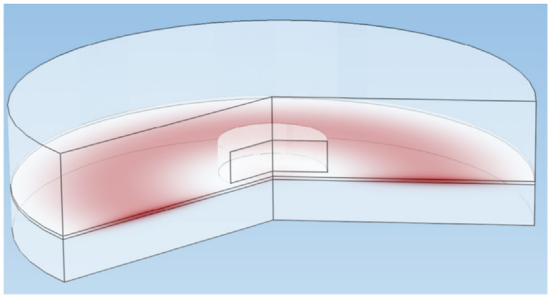

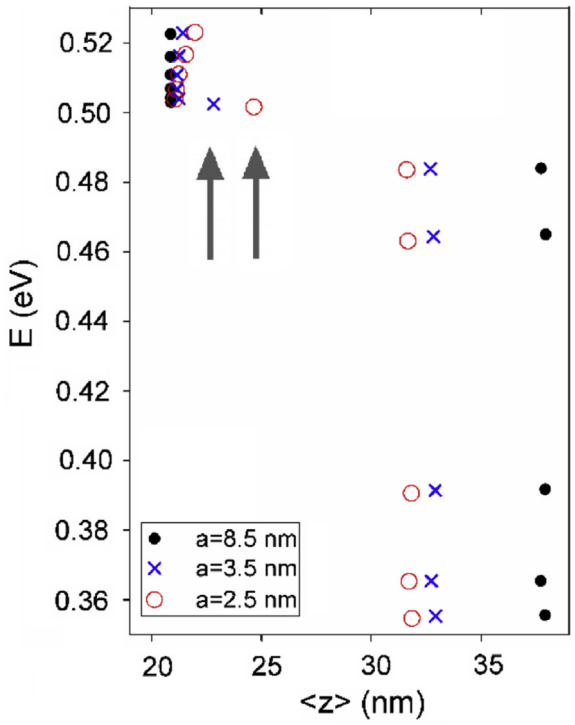

Fig. 4. (Upper) 3D model of the QD-QW complex having the rotation symmetry. The square of the wave function of the electron localized in QW is shown by red color. (Lower) The spectral distribution of localized/delocalized states in 3D InAs/GaAs dot-well complex for different barrier thicknesses a is shown by various symbols along the averaged coordinate $\langle z\rangle$. Electron tunneling occurs through the QW lowest energy level and relates to the delocalized state (noted by the arrow). (For interpretation of the references to color in this figure legend, the reader is referred to the Web version of this article.)

$$\langle x\rangle_- = -\sin^2(\Theta/2)|\langle x\rangle_1| + \cos^2(\Theta/2)|\langle x\rangle_2| - 2\sin(\Theta/2)\cos(\Theta/2)|\langle x\rangle_{12}|,$$

where, $\Theta = arctg(W/\Delta E_{12})$. The parameter W is a coupling coefficient of the quantum system elements, it depends on the wave function overlap for the "unperturbed states" ψ_1 and ψ_2. $\Delta E_{1,2} = E^1_{g.s} - E^2_{g.s.}$ is energy difference of separated left (index 1) and right (index 2) QWs as shown in Fig. 3. The matrix element W (which is also proportional to the quasi-doublet energy splitting ΔE) can be described using the following relation [16]: $W \sim S$, where S is the overlap integral, approximated by $S = \int_\Sigma \psi^2(x,y)dxdy$, with the integration domain Σ being the area between the QWs. It is clear, that the electron localization in DQW is extremely sensitive to small violations of DQW symmetry, when $\Delta E_{12} \approx 0$ [1].

3. Numerical modeling for carrier transfer from the barrier in InAs/GaAs-InGaAs/GaAs dot-well

The tunneling in the hybrid QD-QW complex is considered in

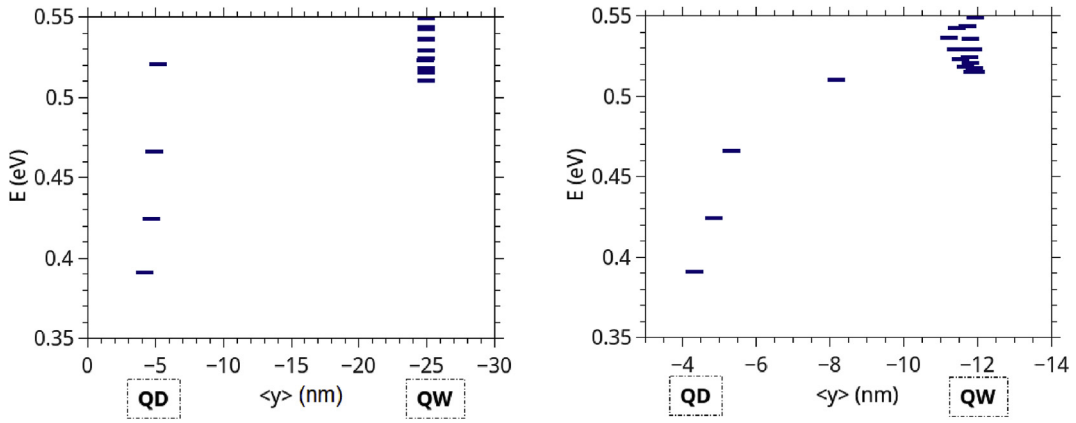

Fig. 5. The spectral distribution of localized/delocalized states in 2D InAs/GaAs dot-well complex for different barrier thicknesses, a. (Left) $a = 20$ nm and there are no delocalized (tunneling) states. (Right) $a = 8$ nm.

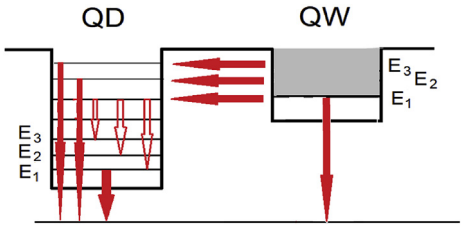

Fig. 6. Schematic description of the PL experiments from Ref. [11]. Electron confinement structure and energy levels. The notations are the same as in Fig. 2.

relation to the PL experiments [10] (see Fig. 2). The QD - QW tunneling has been experimentally indicated by the PL peaks, between the lowest QD and QW peaks, which were observed for separated QD and QW.

The 3D modeling is includes the QD and QW having the rotation symmetry as is shown in Fig. 4(Upper). The Neumann boundary conditions were used for the QW. The results of numerical modeling are given in Fig. 4(Lower) for the spectral distributions of the localized/delocalized states shown for several QD-QW geometries. The tunneling between QW and QD occurs for the lowest energy level of QW quasi-discrete spectrum. This situation is directly comparable with the experimental picture proposed in Ref. [10]. The tunneling is possible for the closely deposited QD and QW. The dependence given in Fig. 4

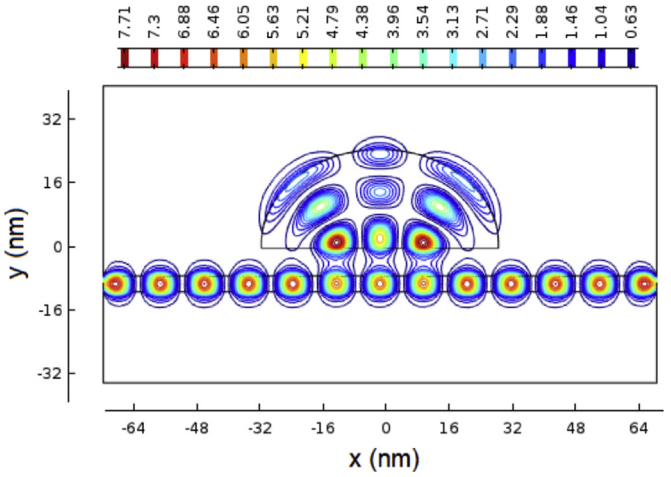

Fig. 8. The square of electron wave function in 2D InAs/GaAs dot-well complex (contour plot). The color legend for the plot is shown. (For interpretation of the references to color in this figure legend, the reader is referred to the Web version of this article.)

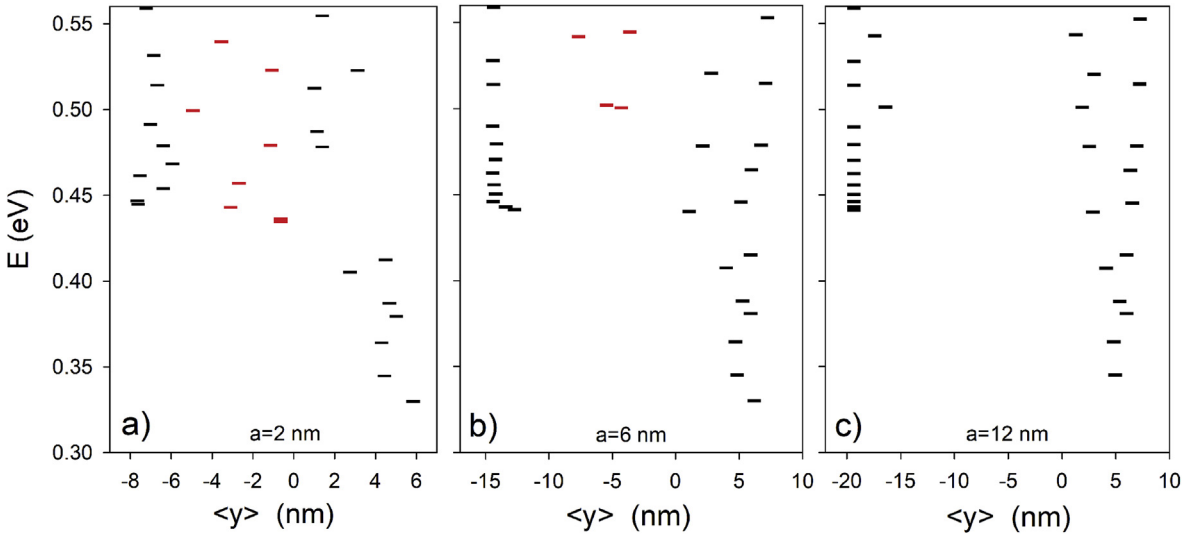

Fig. 7. The spectral distribution of localized/delocalized states in 2D InAs/GaAs dot-well complex for different barrier thicknesses a) $a = 2$ nm, b) $a = 6$ nm and c) $a = 12$ nm. Delocalized states are shown in red color. (For interpretation of the references to color in this figure legend, the reader is referred to the Web version of this article.)

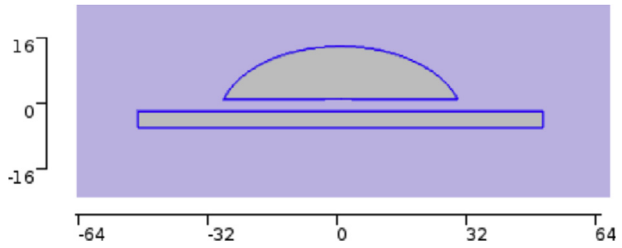

Fig. 9. Geometry of the dot-dot complex (2D model). The sizes are given in nm.

shows that the barrier thickness $a = 8$ nm is critical for the tunneling, which occurs when $a < 8$ nm and is detected for $\langle z \rangle$ in range of [22,30] nm. When $a > 8$ nm, the tunneling is not possible and we see the spectra of separated QD and QW. The spectrum of QD is discrete and electron localizes about $\langle z \rangle \approx 38$ nm. The QW spectrum is quasi-continuous due to numerical approximation and the electron is localized in QW with $\langle z \rangle \approx 21$ nm.

In Fig. 5, we present the results of numerical modeling for tunneling in the 2D-1D QD-QW complex. The geometry of the complex is shown in Fig. 1. One can see in Fig. 5 (Left) that the QD and QW may be described as separated for large barrier thicknesses, the electron spectrum relates to single QD or QW. Corresponding localization is noted as "QD" or "QW" in the figure. The tunneling occurs for the lowest QW level (or higher confinement state of QD) when a decreases to 8 nm and electron is localized in QD and QW, with $\langle y \rangle \approx 9$ nm. This property is again directly related to the experiment [10]. Experiments given in Ref. [11] can be modeled by increasing the size of QD-QW complex. The schematic description of the PL experiments [11] is presented in Fig. 6.

The results of numerical modeling for tunneling in reconfigured 2D-1D QD-QW complex are presented in Fig. 7. The calculations were performed for different values of the barrier thickness a. Once more, one can see that tunneling is possible when the QD and QW are close enough. The tunneling occurs through higher levels of discrete spectrum of QD and low-lying levels of quasi-continuous spectrum of QW. Comparing this result with the QD-QW experiment one can conclude that QW in the experiment has quasi-continuous spectrum too. Our interpretation for this fact is that the region of interaction between QD and QW is local and has a limitation by size of common QD-QW interface B along x-axis (see Fig. 1). The spectral level energy can be evaluated as L^2/B^2, where $L = 1, 2, 3, \ldots$ for each bands generated by the QW thickness. In the calculations shown in Fig. 7, there is one such band. For the QD, there are two such bands $N = 1, 2$. The electron of a different N-band localizes differently as one can see in Fig. 7c) where QD spectrum is splinting to two branches from the lowest states to highest ones.

An approximation for energy of levels can be written as $E_{KN} \sim (K^2/R_x^2 + N^2/R_y^2)$ for the 2D quantum dot. Where R_y (R_x) are effective QD size along y (x) direction. For the QD, we effectively has $N = 1, 2$ due to size limitation and limitation for the energy in the confinement region from 0.33 eV to 55 eV. Increasing the QD y-direction size one can obtain the state with $N = 3$ as it is illustrated in Fig. 8. The wave function of the state is spread over the QD-QW complex with different probability to be in QW or QD. The state presented in Fig. 8 is the delocalized one and electron tunneling may be occurred through this state. It is clear that the averaging over y-coordinate leads to different values of $\langle y \rangle$ for different localized/delocalized states as is shown in Fig. 7 due to variations of the wave function spacial distribution in QD. The number of delocalized states in the spectrum decreases when the barrier thickness increases. $\langle y \rangle$ demonstrate this relation. The levels having intermediate values of $\langle y \rangle$ between the values corresponding to localized states in QD or QW (see Fig. 7c)) relate to delocalized states which are shown in red color in Fig. 7a) and b).

To show that the spectral structure of the QD-QW tunneling can be determined by interaction between QD and "mirror" area on the QW, we calculate spectral distribution of localized/delocalized states for binary complex of QDs, shown in Fig. 9. This complex is the result of reduction of geometry from the QW to QD in the QD-QW system. The results of the numerical modeling are shown in Fig. 10a) and b) where the spectral distributions of localized/delocalized states in double quantum dot (DQD) and in QD-QW complexes are respectively presented. Comparison both results shows obvious correlation. The tunneling states appear in QD-QW complex with the same energies as in DQD system. Thus, the spectral distribution of the QD-QW tunneling has a discrete character as one can see in Fig. 6.

4. Conclusion

We modeled the resonance tunneling in InAs/GaAs QD-QW complex including 2D (3D) and 1D quantum objects in terms of localized/delocalized states of electron confinement spectrum according the

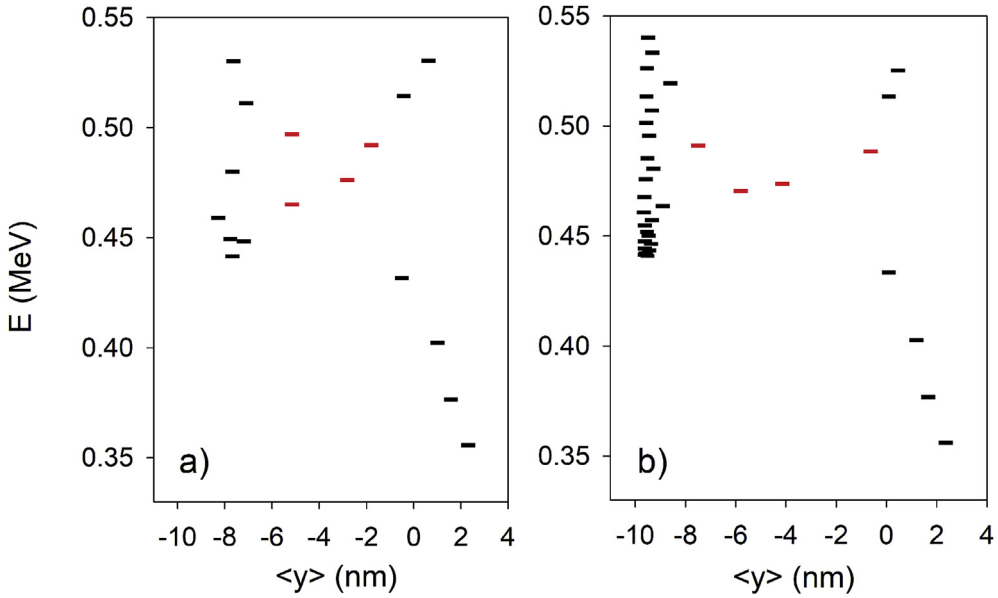

Fig. 10. The spectral distribution of localized/delocalized states in 2D InAs/GaAs a) dot-dot and b) dot-well complexes. The barrier thicknesses $a = 4$ nm. Delocalized states are shown in red color. (For interpretation of the references to color in this figure legend, the reader is referred to the Web version of this article.)

formalism of two-level quantum systems. This modeling covers the main phenomenons of the optical PL experiments given by Yu. I. Mazur et al. in Refs. [10,11]. In particular, we have shown that electron tunneling has discrete distribution along the electron spectrum below and above the lowest level of continuous spectrum of QW. It was shown that the tunneling spectral distribution depends on the geometry factors of the QD-QW complex, which can be predicted by theoretical modeling. We have given the explanation for the discrete nature of the PL spectrum. It was found that the interaction between QD and QW is limited by “mirror” area on the QW. Thus, there is effectively a dot-dot-like complex having discrete spectrum. We can conclude that the optical registration of electron localization in binary quantum systems is possible and has a perspective to be used in new nono-sized devices.

Conflicts of interest

There is no Conflict of interest.

Acknowledgments

This work is supported by the RISE 1829245, DNS 2016-ST-062-000004 and DMR-1523617 awards.

References

[1] I. Filikhin, A. Karoui, B. Vlahovic, Nanosensing backed by the uncertainty principle, J. Nanotechnol. 2016 (2016), https://doi.org/10.1155/2016/3794109 Article ID 3794109.
[2] I. Filikhin, Y.B. Kuzmichev, B. Vlahovic, Electron localization sensitivity in quantum two level systems for nano-sensors, in: S. Yurish (Ed.), SEIA’ 2017 Conference Proceedings, IFSA Publishing, S. L., Barcelona, Spain, 2017, pp. 207–209.
[3] I. Filikhin, S.G. Matinyan, B. Vlahovic, Localized-delocalized states and tunneling in double quantum dots: effect of symmetry violation, Quantum Matter 4 (4) (2015) 358–366, https://doi.org/10.1166/qm.2015.1207.
[4] S.L. Chuang, N.J. Holonyak, Efficient quantum well to quantum dot tunneling: analytical solutions, Appl. Phys. Lett. 80 (2002) 1270, https://doi.org/10.1063/1.1449535.
[5] L.I. Goray, P.N. Racec, Boundary conditions effect on states and transitions in a quantum-well - nanobridge - quantum dot structure, Proceedings of the International Conference DAYS on DIFFRACTION, 2014, pp. 89–95.
[6] W. Rudno-Rudzinski, et al., Room temperature free carrier tunneling in dilute nitride based quantum well - quantum dot tunnel injection system for 1.3 μm, Appl. Phys. Lett. 94 (2009) 171906, https://doi.org/10.1063/1.3122935.
[7] I. Filikhin, V.M. Suslov, M. Wu, B. Vlahovic, InGaAs/GaAs quantum dots within an effective approach, Phys. E Low-Dimens. Syst. Nanostruct. 41 (2009) 1358–1363, https://doi.org/10.1016/j.physe.2009.04.002.
[8] I. Filikhin, V.M. Suslov, B. Vlahovic, Modeling of InGaAs/GaAs quantum ring capacitance spectroscopy in the nonparabolic approximation, Phys. Rev. B 73 (2006) 205332, https://doi.org/10.1103/PhysRevB.73.205332 https://link.aps.org/doi/10.1103/PhysRevB.73.205332.
[9] I. Filikhin, V.M. Suslov, B. Vlahovic, C-V data and geometry parameters of self-assembled InAs/GaAs quantum rings, J. Comput. Theor. Nanosci. 9 (2012) 669, https://doi.org/10.1166/jctn.2012.2077.
[10] Y.I. Mazur, et al., Tunneling-barrier controlled excitation transfer in hybrid quantum dot-quantum well nanostructures, Appl. Phys. Lett. 108 (7) (2010) 074316, https://doi.org/10.1063/1.3493240.
[11] Y.I. Mazur, et al., Excited state coherent resonant electronic tunneling in quantum well-quantum dot hybrid structures, Appl. Phys. Lett. 98 (8) (2011) 083118, https://doi.org/10.1063/1.3560063.
[12] Y.I. Mazur, et al., State filling dependent luminescence in hybrid tunnel coupled dot-well structures, Nanoscale 4 (2012) 7509–7516, https://doi.org/10.1039/C2NR32477F http://dx.doi.org/10.1039/C2NR32477F.
[13] Y.I. Mazur, et al., Effect of tunneling transfer on thermal redistribution of carriers in hybrid dot-well nanostructures, Appl. Phys. Lett. 113 (3) (2013) 034309, https://doi.org/10.1063/1.477968.
[14] D. Guzun, et al., Effect of resonant tunneling on exciton dynamics in coupled dot-well nanostructures, Appl. Phys. Lett. 113 (15) (2013) 154304, https://doi.org/10.1063/1.4801891.
[15] C. Cohen-Tannoudji, B. Diu, F. Laloe, Quantum Mechanics vol. 1, Wiley, 1977.
[16] I. Filikhin, S.G. Matinyan, B. Vlahovic, Tunneling rate in double quantum wells, Sens. Transducers 183 (12) (2014) 116–122 http://www.sensorsportal.com/HTML/DIGEST/P_2551.htm.